Desalination and Water Treatment
www.deswater.com
doi: 10.5004/dwt.2020.24693

173 (2020) 231–242
January

Degradation kinetics of caffeine in water by UV/H_2O_2 and UV/TiO_2

Pedro M. Rendel[a,*], Giora Rytwo[a,b]

[a]*Environmental Physical Chemistry Laboratory, MIGAL, Galilee Research Institute, Kiryat Shmona, Israel, Tel. +972 4 6953568; Fax: +972 4 6944980; emails: prendel@migal.org.il (P.M. Rendel), giorarytwo@gmail.com (G. Rytwo)*
[b]*Department of Environmental Sciences, Tel Hai College, Upper Galilee, Israel*

Received 18 April 2019; Accepted 9 July 2019

ABSTRACT

Considered the world's most widely consumed psychoactive drug, caffeine became a widespread environmental pollutant, contaminating both the hydrosphere as well as the pedosphere, by thus leading to an unclear effect on the surrounding biosphere. Unsuccessfully treated by regular wastewater-treatment plants, caffeine concentrations in discharged effluents and natural reservoirs are constantly rising. New water-treatment technologies are being developed to reduce the concentrations of such emerging contaminants. Photodegradation is recently drawing much attention due to its potential to oxidize such contaminating compounds and its large-scale deployment is still being evaluated. In order to optimize these processes, quantifying and developing new kinetics models are an essential step. In this work, the photodegradation kinetics of caffeine was evaluated under different UV-C doses (1.9–15.2 mJ cm^{-2} s^{-1} and λ = 254 nm) and in the presence of two degradation agents, hydrogen peroxide (H_2O_2) and commercial titanium dioxide (TiO_2) nanopowder. For an initial concentration of 19,600 μg L^{-1} caffeine, the removal rate was higher than 95% for both agents separately, yielding half-life times of 40–5 min for 16.3–163 μmol L^{-1} H_2O_2 and 96–9 min for 1–100 μg L^{-1} TiO_2 suspension, respectively. The degradation rates were governed by pseudo-zero-order reaction kinetics at high caffeine-to-agents ratios (>0.6 for H_2O_2 and >400 for TiO_2), whereas pseudo-first-order kinetics were seen at lower ratios in experiments with TiO_2. Empirical and theoretical rate laws describing the degradation kinetics and their possible mechanism are presented.

Keywords: Caffeine; Kinetics; Photodegradation; Hydrogen peroxide; Titanium dioxide; Wastewater

1. Introduction

Caffeine is a naturally occurring alkaloid and it is considered to be one of the world's most widely consumed psychoactive drugs. It is present in beans, leaves and fruits of more than 60 plant species and it is mostly consumed in beverages such as coffee, tea, mate and energy drinks, as well as in products containing cocoa and chocolate [1].

From an analysis of wastewater, Gracia-Lor et al. [1] estimated the mean daily per capita consumption of caffeine to be as much as 320 mg d^{-1}. Due to this high consumption, traces of caffeine can even be found in remote natural water sources, and thereby its presence is frequently used as an anthropogenic marker for wastewater contamination [2–4].

Caffeine was widely identified in seawater at coastal and marine environments around the world [5,6], consequently rising concerns regarding its potential effect on natural ecosystems, as well as aquaculture and seawater desalination. Such concerns intensify in arid countries where seawater desalination constitutes a fundamental portion of their drinking water supply.

With the wide recognition of caffeine and other pharmaceutical and personal care products as emerging contaminants in the aquatic environment [7–9] with an increasing demand to combine innovative and complementary water-treatment technologies in existing municipal wastewater-treatment plants to reduce the concentrations of emerging

* Corresponding author.

Current address: Technical University of Denmark, DTU, 2800 Kgs., Lyngby, Denmark.
email: prendel@dtu.dk (P.M. Rendel).

contaminants from the effluents. Thus, a detailed evaluation of the degradation kinetics of such contaminants is essential to optimize and scale-up recently developed technologies.

Caffeine degradation is widely used as a preliminary marker to evaluate new degradation technologies for emerging organic contaminants during water- and waste-treatment processes, and has been extensively studied in recent years. While some of the recent studies in the field present unconventional processes developed to degrade caffeine in aquatic solutions, such as methanogenesis [10], photo-Fenton [11] and biodegradation [12], most work has concentrated on the use of advanced oxidation processes (AOPs) to tackle caffeine-contaminated water. AOPs rely mainly on the production of reactive hydroxyl radicals (•OH) in a solution; these acts as a strong oxidant, virtually oxidizing any compound present in the water matrix. The radical-production mechanism strongly depends on the type of AOP being applied. Two of the most widespread mechanism for radical production are (i) heterogeneous photocatalytic oxidation, in which the catalyst and substrate are in different phases. In this process a mineral surface, or an oxide nanopowders (e.g., cobalt nanosheets, titania nanotubes, titanium dioxide (TiO_2), zinc oxide (ZnO), potassium monopersulfate ($KHSO_5$), iron oxyhydroxide ($Fe(OH)_3$), etc.), or specifically synthesized metal/non-metal nanohybrid structures (C_3N_4/UiO-66, MoS_2/MIL-53(Fe) nanosheets, etc.) are introduced into the solution in the presence of UV-A, UV-B or UV-C radiation; irradiation of the photocatalytic surface leads to the formation of an excited electron (e^-) and an electron gap (h^+); water is being adsorbed onto the catalyst surface resulting in dissociation of the water molecule by the highly reactive electron gap, thereby releasing •OH into the solution (e.g. [13–20]); (ii) homogeneous UV/hydrogen peroxide (H_2O_2) oxidation, in which the degradation agent and the substrate are dissolved in the solution. In this process, homolytic cleavage of the O–O bond of H_2O_2 leads to the formation of two •OH radicals [17,21–29].

In this study, we evaluated the degradation kinetics of caffeine experimentally, and established new empirical and theoretical rate laws that describe the degradation kinetics at various UV-C doses (1.9–15.2 mJ cm^{-2} s^{-1} and λ = 254 nm) in the presence of two different degradation agents: H_2O_2 and commercial TiO_2 nanopowder, while TiO_2 behaves as a catalyst and partial participation of H_2O_2 as reactant was not completely neglected thus we prefer to focus on the term "degradation" instead of "catalysis".

2. Theoretical background

2.1. Homogeneous UV/H_2O_2 photodegradation kinetics

Two degradation mechanisms take place simultaneously during homogeneous UV/H_2O_2 photodegradation: (i) photolysis, in which UV radiation alone acts as a degrading agent and (ii) hydroxyl radical reactions, in which the formed •OH in the solution oxidizes the contaminating compound present in the water matrix [25].

Wols et al. [22,25] presented a dynamic kinetic model describing a linear relation between the kinetics of the UV/H_2O_2 degradation process and UV dose H' [mJ cm^{-2} s^{-1}] using a monochromatic UV source, on where the degradation rate coefficient k [cm^2 mJ^{-1}] is expressed by the sum of the photolysis (k_{photo}) and oxidation (k_{ox}) coefficients as follows:

$$\upsilon = kH' = \left(k_{photo} + k_{ox}\right)H' = \left(\ln(10)\frac{\phi\varepsilon}{U_{254}} + 2\ln(10)\frac{\phi_H\varepsilon_H}{U_{254}}\frac{k_c\left[H_2O_2\right]}{\sum\left(k_i\left[C_i\right]\right)+k_H\left[H_2O_2\right]}\right)H' \quad (1)$$

In Eq. (1), ν represents the degradation rate, Φ the quantum yield [mol $Einstein^{-1}$], ε the molar absorption coefficient [L mol^{-1} cm^{-1}], U_{254} the energy of a mole of photons at 254 nm (4.71×10^5 J $Einstein^{-1}$), $\Sigma(k_i[C_i])$ the •OH radical scavenging of deionized water [s^{-1}], k_c the •OH radical reaction rate constant with the target compound [mol L^{-1}], and the subscript H stands for H_2O_2.

2.2. Heterogeneous UV/TiO_2 photocatalytic degradation kinetics

Despite the oversimplification of kinetics models based on "rate determination step" or "steady state" approximations, those can be useful to understand the elementary steps of a complex process. As the TiO_2 degradation reaction is considered to be controlled by surface adsorption mechanisms [30], we proposed and tested two possible mechanisms which might account for such degradation rate:

("α") Adsorption → excitation of the complex → degradation

("γ") Excitation of catalyst → formation of the excited complex during adsorption → degradation

The overall rate of the process is the rate of formation of products. If a simplified approach of "steady state" on the intermediate products is assumed, process "α" (as fully developed in Appendix A) leads to an overall rate of:

$$\upsilon = \frac{d[P]}{dt} = \frac{k_4k_{\alpha 2}k_{\alpha 1}[h\upsilon][T]}{k_{X'} + k_{Y'}[h\upsilon] - k_3k_{\alpha 2}[h\upsilon]}[F] \quad (2)$$

where [F], [T], and [$h\nu$] are the concentrations of caffeine, TiO_2 and, the excitation light, respectively. All other parameters (k_4,$k_{\alpha 2}$,$k_{\alpha 1}$,$k_{X'}$,$k_{Y'}$,k_3) are rate coefficients related to the elementary steps of the process. According to Eq. (2), the proposed process "α" should be a first-order process for caffeine at all concentrations. At high light rates, when $k_{X'}/(k_{Y'} - k_3k_{\alpha 2}) \ll [h\upsilon]$, the proposed process will apparently become pseudo-zero-order on light intensity.

Adopting the same "steady state" approximation, process "γ", on the other hand, leads to an overall rate described by:

$$\upsilon = \frac{d[P]}{dt} = k_4k_{\gamma 1}k_{\gamma 2}[h\upsilon][T]\frac{[F]}{\left(k_X + k_Y[F]\right)} \quad (3)$$

for which parameters (k_4,$k_{\gamma 1}$,$k_{\gamma 2}$,k_X,k_Y) are rate coefficients related to the elementary steps of process "γ". Interestingly, as described in Appendix A, process "γ" will behave as a

pseudo-first- and pseudo-zero-order process for low and high caffeine concentrations, respectively. Thus, measured results might indicate which of the mechanisms better describes the heterogeneous photodegradation of the caffeine.

3. Methods

The degradation kinetics of caffeine was evaluated by performing a series of batch experiments in a mini photochemical chamber reactor. Caffeine solution was exposed to UV-C radiation (254 nm wavelength) in the presence of two different degradation agents: H_2O_2 and the commercial TiO_2 nanopowder (Hombikat®, L.A. CA, USA) at intensities ranging from 1.9 to 15.2 mJ cm^{-2} s^{-1} in the UV-C range. The detailed experimental plan is presented in Table S1.

3.1. Experimental solutions

Caffeine and TiO_2 bulk solutions were prepared by dissolving/mixing weighed amount of caffeine or fine crystalline catalyst-grade industrial TiO_2 (Hombikat®, L.A. CA, USA) powders (Sigma-Aldrich, St. Louis, Missouri, USA) in deionized water, for the solutions between 1.96 and 10 g L^{-1}, respectively. The H_2O_2 bulk solution was prepared by diluting a 30% (9.79 M) concentrated H_2O_2 solution (Merck, Darmstadt, Germany) in deionized water to a final 5% (1.63 M) H_2O_2 solution.

During the experiments, 1 mL of caffeine bulk solution was poured into 99 mL of deionized water for a final solution concentration of 19,600 μg L^{-1} (100 μM). Different volumes of the degradation agents solutions (TiO_2 and H_2O_2) were added, as further described in Table S1, yielding a TiO_2 suspension of 10–200 μg L^{-1}, and H_2O_2 concentrations of 16.3–163 μmol L^{-1} (0.55–5.54 mg L^{-1}).

3.2. Experimental setup

Experimental solutions were poured into a 100 mL UV-C-transparent quartz glass (refractive index n = 1.5048) beaker and placed in a Rayonet RMR-600 mini photochemical chamber reactor (Southern New England Ultraviolet Company, Branford, CT, USA) with an optical path length of 5.3 cm (Fig. 1). The chamber was equipped with eight RMR 2537A lamps (254 nm wavelength), each lamp emitting an irradiance flux of 1.9 mJ cm^{-2} s^{-1} at 254 nm, as measured in the center of the chamber using a Black Comet SR spectrometer (StellarNet Inc., Tampa, FL) with an F400 UV-VIS-SR-calibrated fiber optic probe equipped with a CR2 cosine light receptor. The solution was constantly mixed with an external impeller driven by an overhead stirrer motor (VELP Scientifica, Usmate Velate, Italy) rotating at 100 rpm. To obtain different UV doses, part of the lamps were disconnected, giving 50%, 25% and 12.5% of the original UV dose.

Periodically, every 1.5 to 10 min, approximately 1 mL solution was drawn from the beaker for UV-VIS spectroscopy measurement of caffeine concentration (Hewlett Packard 8452A diode array spectrophotometer driven by Chemstation 06.03 software, Palo Alto, CA, USA). Evaluation was performed at 272 nm (molar absorption coefficient ε = 10,750 M^{-1} cm^{-1}) using absorbance at 320 nm for baseline correction. In experiments, where the TiO_2 catalyst suspension was >30 μg L^{-1}, samples were centrifuged at 13,000 rpm (SciLogex D2012, Rocky Hill, CT, USA) for 17 min prior to the UV-VIS spectroscopy measurement to eliminate light dispersion caused by the suspended nanoparticles. The uncertainties of the measurements were estimated at less than 3%.

3.3. Apparent rate coefficient calculations

Considering all parameters (e.g., catalyst/degradation agent concentration, irradiation rate, temperature, etc.) as constant, the contaminating compound degradation can be defined by a simple rate law:

$$\upsilon = \frac{d[C]}{dt} = k_{app}[C]^{n_{app}} \tag{4}$$

Fig. 1. Experimental setup.

where ν is the reaction rate, k_{app} is the apparent rate coefficient, C is the degrading compound concentration and n_{app} is the apparent or "pseudo" reaction order. n_{app} can be found empirically and is related to the mechanism by which the process occurs. The term "pseudo" is used to acknowledge the fact that all other influencing parameters (catalyst/degradation agent, temperature, light, etc.) were kept constant, either actually (as in catalysts) or virtually (their initial concentration was so large that the change in concentration was insignificant) [31].

To simplify the calculations and allow comparisons between parameters in different reaction mechanisms, the "relative concentration at time t" (A) was defined as C_t/C_0 (the ratio of actual to initial concentration); thus $A_0 = 1$. Since A is dimensionless, none of the parameters have concentration units. This is convenient since it yields apparent kinetic coefficients that always have dimensions per time, regardless of the order of the process [18]. Specific rate laws for pseudo-zero and first-order kinetics are shown in Appendix B.

4. Results and discussion

4.1. Caffeine degradation by UV-C/H_2O_2 and UV-C/TiO_2

4.1.1. Caffeine degradation as a function of H_2O_2 and TiO_2 concentration

The degradation of caffeine as a function of various H_2O_2 and TiO_2 concentrations is shown in Figs. 2 and 3, respectively. In most of the experiments, the removal rate of ca. 95% was observed (further degradation was not evaluated due to analytical limitations). No degradation was observed when H_2O_2 or TiO_2 was applied without activating the UV-C source, or conversely when activating the UV-C source without a degradation agent. The linear decrease in the relative concentration with time implies degradation processes that follow pseudo-zero-order kinetics Eq. (A1) for both agents. The obtained apparent rate coefficient k_{app} tended to increase with rising H_2O_2 and TiO_2 concentrations for half-life times ranging between 40 and 5 min for H_2O_2 concentrations of 16.3–163 μmol L^{-1} and between 96 and 9 min for a TiO_2 suspension of 1–100 μg L^{-1}, respectively. The apparent rate coefficients and half-life times are fully detailed in Table S1.

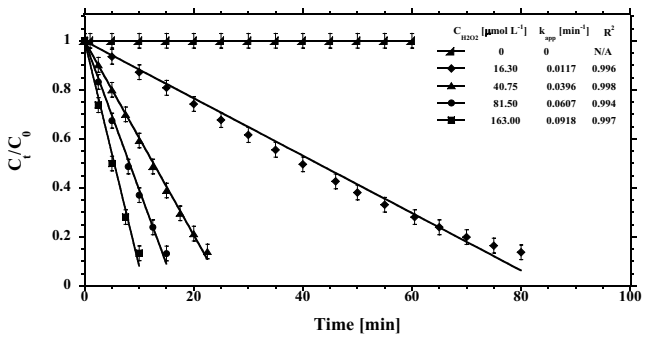

Fig. 2. Degradation of caffeine vs. time, at various H_2O_2 concentrations (0–163 μmol^{-1}). Different symbols represent measured values (duplicates) at different H_2O_2 concentrations whereas lines were evaluated for pseudo-zero-order kinetics with apparent rate coefficients k_{app} as described in the figure.

4.1.2. Effect of UV dose

Various UV-C doses in experiments containing different H_2O_2 and TiO_2 concentrations were evaluated to quantify their effect on the caffeine-degradation rate. UV-C lamps were sequentially removed from the photochemical chamber reactor, providing different UV-C doses. The fraction of the applied UV-C dose (H') is represented by the parameter β, which for the maximum dose (eight active lamps) H' = 15.2 mJ cm^{-2} s^{-1}, it is equal to 1.

Results from two representative sets of experiments with constant concentrations of H_2O_2 (163 μmol L^{-1}) and TiO_2 (20 μg L^{-1}) are shown in Figs. 4 and 5, respectively. Caffeine-degradation rate slowed with decreasing applied UV-C dose, as expected, but the process still showed a good fit to pseudo-zero-order kinetics. This implies that under the presented experimental conditions, UV-C radiation is not a limiting factor, but may become one at very low UV-C intensities as insinuated by the convex dots around the pseudo-zero-order regression line at β = 0.125. The obtained apparent rate coefficients and half-life times are detailed in Table S1.

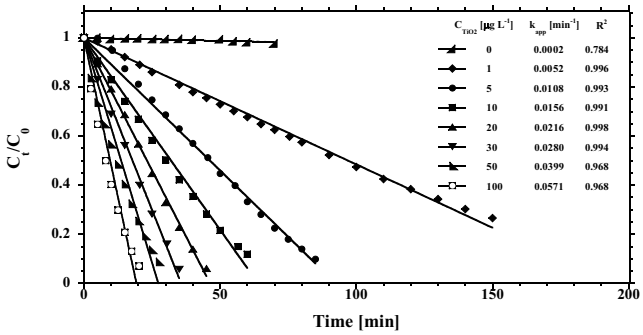

Fig. 3. Degradation of caffeine vs. time, with various TiO_2 suspensions (0–100 μg L^{-1}). Different symbols represent measured values (duplicates) for different TiO_2 suspensions whereas lines were evaluated for pseudo-zero-order kinetics with apparent rate coefficients k_{app} as described in the figure.

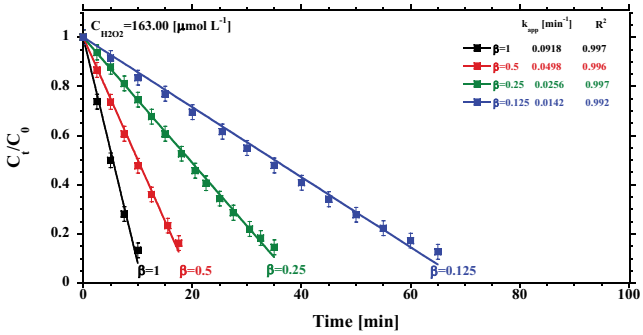

Fig. 4. Degradation of caffeine vs. time at different UV-C doses (dose fraction β ranging from 1 to 0.125, represented by the different colors) in the presence of 163 μmol L^{-1} H_2O_2. Squares are measured values whereas lines represent fit to a zero-order model with apparent rate coefficients, k_{app}, as described in the figure.

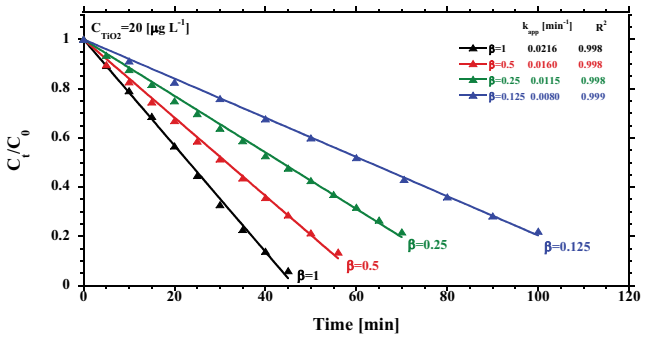

Fig. 5. Degradation of caffeine vs. time, at different UV-C doses (dose fraction β ranging from 1 to 0.125, represented by the different colors) in the presence of 20 μg L^{-1} TiO_2. Triangles are measured values whereas lines represent fit to a zero-order model with apparent rate coefficients, k_{app}, as described in the figure.

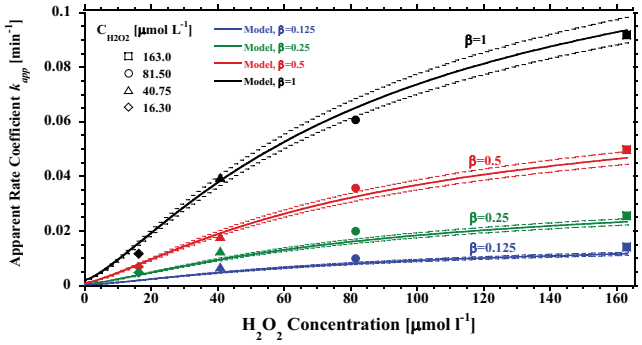

Fig. 6. Experimental and calculated apparent rate coefficients (k_{app}) vs. H_2O_2 concentration (represented by different symbols) at different UV-C doses (represented by β with different colors). Solid and dashed lines represent the theoretical model prediction and a 5% uncertainty envelope, respectively; dots represent experimental results.

4.1.3. Degradation kinetics

Previous works reported a pseudo-first-order reaction rate for caffeine degradation rather than pseudo-zero-order kinetics [17,21]. The obtained reaction orders may be influenced by the initial caffeine-to-degradation agent ratio in the solution [21]. It is thus suggested that the obtained pseudo-zero-order kinetics in the present work might be accounted for by the relatively high initial caffeine-to-degradation agent ratios used (6.13–0.6 for H_2O_2 and 80–8,000 for TiO_2) compared to previously reported ratios (0.6–0.01 for H_2O_2 [17,21], and 1.25 × 10^{-6} for TiO_2 [32]).

4.1.4. Kinetic model for the UV-C/H_2O_2 system

The degradation rates of caffeine in the presence of different H_2O_2 concentrations and UV-C doses obtained in this study can be accounted by a previously described first-order dynamic kinetic model [22,25] with slight modifications (Eq. (1)). This model was originally aimed at describing degradation rates only during early stages of the reaction when the rate is not influenced by the contaminating compound's initial concentration, similar to pseudo-zero-order kinetics, which is also independent of the initial compound concentration. Thus, in our case, the model can predict the rate during the whole reaction.

$$\text{Rate} = k^{\alpha}\beta = (k_{photo}k_{ox})^{\alpha}\beta = \left(\ln(10)\frac{\phi\varepsilon}{U_{254}} + 2\ln(10)\frac{\phi_H\varepsilon_H}{U_{254}}\frac{k_c[H_2O_2]}{\sum(k_i[C_i]) + k_H[H_2O_2]}\right)^{\alpha}\beta \quad (5)$$

The sole effect of UV radiation (i.e., photolysis) on caffeine degradation can be evaluated by the value of the photolytic rate coefficient k_{photo}. Applying the values of caffeine's quantum yield Φ (0.18 × 10^{-2} mol Einstein^{-1}) and molar absorption coefficient ε (3.92 × 10^3 L mol^{-1} cm^{-1}) both at 254 nm, was previously reported by Wols and Hofman-Caris [25], yields a k_{photo} value of 3.45 × 10^{-5} cm^2 mJ (U_{254} = 4.71 × 10^{-5} J Einstein^{-1}), thus making a relatively negligible contribution to the overall rate. This result is reinforced by our reported observations as well as those reported by others [21].

Other values reported by Wols et al. [22] and Wols and Hofman-Caris [25] were used to evaluate the contribution of the oxidation process to the degradation rate: H_2O_2 quantum yield at 254 nm Φ_H = 0.5 mol Einstein^{-1}, H_2O_2 molar absorption coefficient at 254 nm ε_H = 18.6 L mol^{-1} cm^{-1}, •OH rate constant k_H = 2.7 × 10^7 L mol^{-1} s^{-1} •OH scavenging of deionized water $\Sigma(k_i[C_i])$ = 1.6 × 10^3 s^{-1} and the •OH reaction rate constant k_c = 6.4 ± 0.7 × 10^9 L mol^{-1} s^{-1}.

A single fitting coefficient α = 1.56, was applied in the model equation to compensate for different physical discrepancies that might arise in the coefficients due to the different experimental environments used during their determination. The modeling and experimental behaviors of the apparent rate coefficients k_{app} as a function of H_2O_2 concentration and in the presence of different UV-C doses are shown in Fig. 6. Accordingly, Fig. 7 shows the agreement between the experimental and modeling results.

4.1.5. Kinetic model for the UV-C/TiO_2 system

Similar to the case of H_2O_2 as a degradation agent, with TiO_2 the degradation rates showed pseudo-zero-order kinetics; a new empirical rate law which predicts pseudo-zero-order kinetics caffeine-degradation rates in the presence of TiO_2 catalyst at various UV-C doses was determined:

$$\text{Rate} = k_{app} = \left(4.83\times10^{-3}\right)\times\left\{[T]\times\beta\right\}^{0.5} \quad (6)$$

where k_{app} is the apparent rate coefficient (min^{-1}), β is the fraction of the applied UV-C dose, and T is the concentration of TiO_2 catalyst in suspension [μg L^{-1}].

The calculated vs. experimental k_{app} values as a function of TiO_2 concentration and different UV-C doses are shown in Fig. 8.

An attempt was made to determine the transit range over which the reaction order may transgress from pseudo-zero-order to pseudo-first-order kinetics.

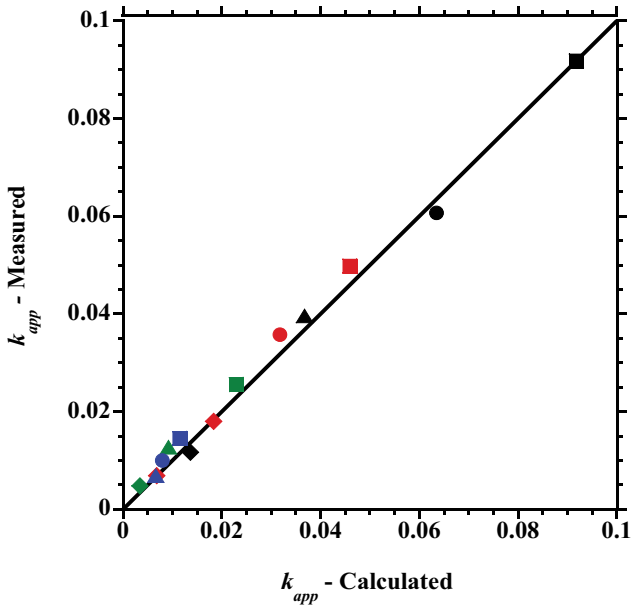

Fig. 7. Agreement between the experimental and modeled apparent rate coefficients (k_{app}). Symbols and colors according to the legend for Fig. 6.

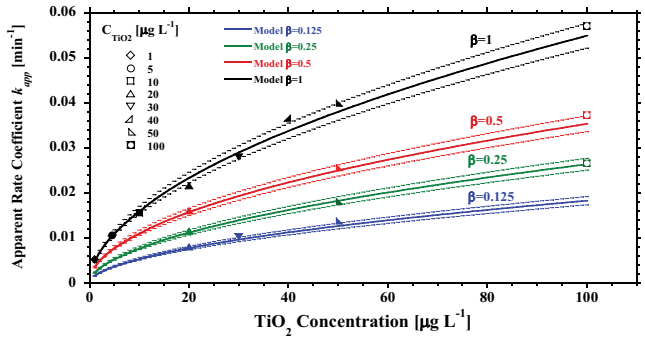

Fig. 8. Experimental and calculated apparent rate coefficients (k_{app}) vs. TiO_2 suspension (represented by different symbols) at different UV-C doses (represented by β with different colors). Solid and dashed lines represent the theoretical model prediction and a 5% uncertainty envelope, respectively, while dots represent experimental results.

Two sets of caffeine-degradation experiments with decreasing caffeine-to-TiO_2 ratios were performed. In the first set of experiments, different TiO_2 catalyst suspensions (ranging from 10 to 200 μg L^{-1}) were applied, to a constant 9,800 μg L^{-1} caffeine solution (Figs. 9a and c). In the second set of experiments, a constant suspension of TiO_2 (200 μg L^{-1}) was used in solutions with different caffeine concentrations (ranging from 9,800 to 24,500 μg L^{-1}) (Figs. 9b and d).

As indicated by the R^2 index value presented in Fig. 9a, increasing disagreement between the data points and a zero-order kinetics regression was obtained as the caffeine-to-TiO_2 ratio decreased, and agreement with first-order kinetics is observed in Fig. 9c, implying that degradation rates in experiments with caffeine-to-TiO_2 ratios smaller than ~300–400 show first-order kinetics, while higher values show zero-order kinetics. Thus, this caffeine-to-TiO_2 ratio range may be treated as a transit range between pseudo-zero- and first-order kinetics.

During the second set of experiments described in Figs. 9b and d, the caffeine-to-TiO_2 ratio was kept below the transit range, producing only first-order reaction kinetics as shown by the higher R^2 values in Fig. 9d compared to Fig. 9b.

Referring to the possible reaction mechanisms described in section 2.2, these results imply that the order of the photons and TiO_2 is not as expected by the collision mechanism "α" which does not fit the measured results in two aspects:

- According to Eq. (A12) in Appendix A, the proposed process should be first order for caffeine at all concentrations.
- At high light rates, when $k_{X'}/(k_{Y'} - k_3 k_{\alpha 2}) \ll [h\upsilon]$ the proposed process should apparently become pseudo-zero-order on light intensity, and this effect was not observed.

A more complex mechanism, yielding for both order of the photons and the TiO_2 suspensions, a ½ pseudo-order will influence only the rate law of the formation of $[T^*]$ (process [γ1], Eq. (A13) in Appendix A), and its rate will become $k_{\gamma 1}[h\nu]^{0.5}[T]^{0.5}$. This will only influence Eq. (7):

$$\frac{d[T^*]}{dt} = k_{\gamma 1}[h\upsilon]^{0.5}[T]^{0.5} - k_{\gamma -1}[T^*] - k_{\gamma 2}[T^*][F] \tag{7}$$

and the overall rate will become

$$\upsilon = \frac{d[P]}{dt} = k_4 k_{\gamma 1} k_{\gamma 2}[h\upsilon]^{0.5}[T]^{0.5}\frac{[F]}{(k_X + k_Y[F])} \tag{8}$$

Thus, such behavior is based on a process where the catalyst first adsorbs a photon and becomes excited, and only afterward does the caffeine is bind to the excited catalyst, leading to degradation, which fits the measured results.

5. Summary and conclusions

The degradation rate of caffeine was studied in a series of batch experiments in the presence of different UV-C radiation doses and two different degradation agents: homogeneous degradation by H_2O_2 and heterogeneous catalysis by TiO_2. Experimental results showed a higher than 95% caffeine-removal rate using either agent separately. Half-life times in caffeine solutions (19,600 μg L^{-1}) ranged between 40 and 5 min for H_2O_2 concentrations from 16.3 to 163 μmol L^{-1} and between 96 and 9 min for TiO_2 suspensions from 1 to 100 μg L^{-1}, respectively.

With both degradation agents, the degradation rates were governed by pseudo-zero-order kinetics at high caffeine-to-degradation agent ratios (>0.6 for H_2O_2, and >400 for TiO_2), while first-order kinetics was seen at lower ratios in experiments with TiO_2. A transit range between pseudo-zero- and first-order reactions was shown to exist at caffeine-to-TiO_2 ratios in the range from 300 to 400.

UV-C intensity was found to play an important role in degradation kinetics but was not found to be a limiting

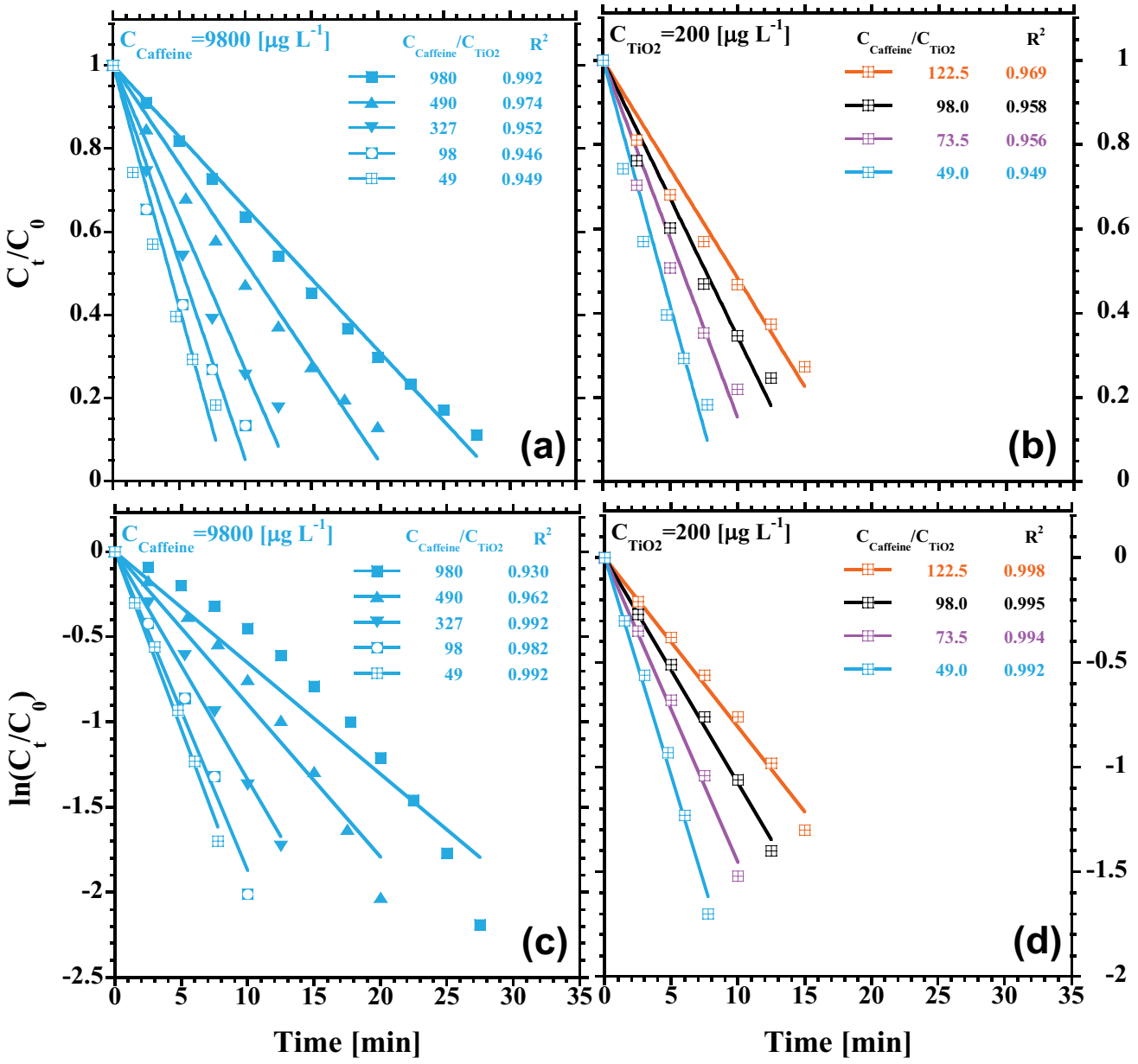

Fig. 9. Experimental results of low caffeine-to-TiO_2 ratio experiments. Linear regressions represent agreement with pseudo-zero-order kinetics in (a) and (c) and pseudo-first-order kinetics in (b) and (d). Symbols represent different TiO_2 suspensions and colors represent different caffeine concentrations.

factor during the reaction under the presented experimental conditions.

A slightly modified dynamic kinetic model (Eq. (5)) based on the previously described model by Wols and Hofman-Caris [25] was found to accurately predict the degradation rate of caffeine in the presence of H_2O_2 at different UV-C intensities.

An empirical model was found to accurately predict the degradation rate of caffeine in the presence of TiO_2 at different UV-C intensities at a caffeine-to-TiO_2 ratio <400. A mechanism based on the widely used "steady state approximation", in which the catalyst first absorbs a photon and becomes excited, and only afterward the caffeine binds to the excited catalyst leading to degradation, fits the measured results. Such theoretical model suggests a reasonable explanation for the transit range within which the reaction order transgresses from zero-order kinetics for experiments with low caffeine-to-TiO_2 ratios to first-order kinetics at experiments with high caffeine-to-TiO_2 ratios.

Various degradation pathways for caffeine degradation were suggested in previous works [15,16,20,33], yet, some discrepancies exist between the different suggested pathways, as they may be largely influenced pending on the applied degradation method. Ongoing work is performed

in order to determine the degradation pathway by means of liquid chromatography-mass spectrometry.

The presented models and parameters can be easily applied to estimate process efficiency. Nevertheless, further research is needed to accurately assess additional parameters, such as cost efficiency, efficacy of the process in a complex matrix including several dissolved components, ionic strength, suspended particles from either biological or mineral sources, and most importantly, to confirm the achievement of full mineralization or at least lack of hazardous by-product formation.

Acknowledgments

This research was supported by a MIGAL internal grant. We would like to express our gratitude to J. Borzenko and C. Michaeli for their technical assistance and to Mrs. Camille Vainshtein for her professional English editing.

References

[1] E. Gracia-Lor, N.I. Rousis, E. Zuccato, R. Bade, J.A. Baz-Lomba, E. Castrignanò, A. Causanilles, F. Hernández, B. Kasprzyk-Hordern, J. Kinyua, A.-K. McCall, A.L.N. van Nuijs, B.G. Plósz, P. Ramin, Y. Ryu, M.M. Santos, K. Thomas, P. de Voogt, Z. Yang, S. Castiglioni, Estimation of caffeine intake from analysis of caffeine metabolites in wastewater, Sci. Total Environ., 609 (2017) 1582–1588.

[2] I.J. Buerge, T. Poiger, M.D. Müller, H.R. Buser, Caffeine, an anthropogenic marker for wastewater contamination of surface waters, Environ. Sci. Technol., 37 (2003) 691–700.

[3] R. Linden, M.V. Antunes, L.S. Heinzelmann, J.D. Fleck, R. Staggemeier, R.B. Fabres, A.D. Vecchia, C.A. Nascimento, F.R. Spilki, Caffeine as an indicator of human fecal contamination in the Sinos River: a preliminary study, Braz. J. Biol., 75 (2015) 81–84.

[4] E.S. Gonçalves, S.V. Rodrigues, E.V. da Silva-Filho, The use of caffeine as a chemical marker of domestic wastewater contamination in surface waters: seasonal and spatial variations in Teresópolis, Brazil, Rev. Ambient. Água, 12 (2017) http://dx.doi.org/10.4136/ambi-agua.1974.

[5] R. Dafouz, N. Cáceres, J.L. Rodríguez-Gil, N. Mastroianni, M. López de Alda, D. Barceló, Á.G. de Miguel, Y. Valcárcel, Does the presence of caffeine in the marine environment represent an environmental risk? a regional and global study, Sci. Total Environ., 615 (2018) 632–642.

[6] K. Nödler, D. Voutsa, T. Licha, Polar organic micropollutants in the coastal environment of different marine systems, Mar. Pollut. Bull., 85 (2014) 50–59.

[7] B. Petrie, R. Barden, B. Kasprzyk-Hordern, A review on emerging contaminants in wastewaters and the environment: current knowledge, understudied areas and recommendations for future monitoring, Water Res., 72 (2015) 3–27.

[8] A.J. Ebele, M. Abou-Elwafa Abdallah, S. Harrad, Pharmaceuticals and personal care products (PPCPs) in the freshwater aquatic environment, Emerg. Contam., 3 (2017) 1–16.

[9] R. Loos, R. Negrão De Carvalho, S. Comero, D.S. Conduto António, M. Ghiani, T. Lettieri, G. Locoro, B. Paracchini, S. Tavazzi, B. Gawlik, L. Blaha, B. Jarosova, S. Voorspoels, D. Schwesig, P. Haglund, J. Fick, O. Gans, EU wide monitoring survey on waste water treatment plant effluents, Institute for Environment and Sustainability, JRC Sci. Policy Rep., (2012) doi:10.2788/60663.

[10] R. Chen, H.Y. Jiang, Y.-Y. Li, Caffeine degradation by methanogenesis: efficiency in anaerobic membrane bioreactor and analysis of kinetic behavior, Chem. Eng. J., 334 (2018) 444–452.

[11] A.G. Trovó, T.F.S. Silva, O. Gomes Jr., A.E.H. Machado, W.B. Neto, P.S. Muller Jr., D. Daniel, Degradation of caffeine by photo-Fenton process: optimization of treatment conditions using experimental design, Chemosphere, 90 (2013) 170–175.

[12] S. Nanjundaiah, S. Mutturi, P. Bhatt, Modeling of caffeine degradation kinetics during cultivation of *Fusarium solani* using sucrose as co-substrate, Biochem. Eng. J., 125 (2017) 73–80.

[13] M.K. Arfanis, P. Adamou, N.G. Moustakas, T.M. Triantis, A.G. Kontos, P. Falaras, Photocatalytic degradation of salicylic acid and caffeine emerging contaminants using titania nanotubes, Chem. Eng. J., 310 (2017) 525–536.

[14] A. Elhalil, R. Elmoubarki, A. Machrouhi, M. Sadiq, M. Abdennouri, S. Qourzal, N. Barka, Photocatalytic degradation of caffeine by ZnO-$ZnAl_2O_4$ nanoparticles derived from LDH structure, J. Environ. Chem. Eng., 5 (2017) 3719–3726.

[15] K.Y.A. Lin, H.K. Lai, S. Tong, One-step prepared cobalt-based nanosheet as an efficient heterogeneous catalyst for activating peroxymonosulfate to degrade caffeine in water, J. Colloid Interface Sci., 514 (2018) 272–280.

[16] F. Qi, W. Chu, B.B. Xu, Catalytic degradation of caffeine in aqueous solutions by cobalt-MCM41 activation of peroxymonosulfate, Appl. Catal., B, 134–135 (2013) 324–332.

[17] J. Rivas, O. Gimeno, T. Borralho, J. Sagasti, UV-C and UV-C/peroxide elimination of selected pharmaceuticals in secondary effluents, Desalination, 279 (2011) 115–120.

[18] G. Rytwo, T. Klein, S. Margalit, O. Mor, A. Naftali, G. Daskal, A continuous-flow device for photocatalytic degradation and full mineralization of priority pollutants in water, Desal. Wat. Treat., 57 (2015) 16424–16434.

[19] O. Sacco, V. Vaiano, M. Matarangolo, ZnO supported on zeolite pellets as efficient catalytic system for the removal of caffeine by adsorption and photocatalysis, Sep. Purif. Technol., 193 (2018) 303–310.

[20] J. Wang, Y.B. Sun, H. Jiang, J.W. Feng, Removal of caffeine from water by combining dielectric barrier discharge (DBD) plasma with goethite, J. Saudi Chem. Soc., 21 (2017) 545–557.

[21] Z.Q. Shu, J.R. Bolton, M. Belosevic, M. Gamal El Din, Photodegradation of emerging micropollutants using the medium-pressure UV/H_2O_2 advanced oxidation process, Water Res., 47 (2013) 2881–2889.

[22] B.A. Wols, C.H.M. Hofman-Caris, D.J.H. Harmsen, E.F. Beerendonk, Degradation of 40 selected pharmaceuticals by UV/H_2O_2, Water Res., 47 (2013) 5876–5888.

[23] B.A. Wols, D.J.H. Harmsen, J. Wanders-Dijk, E.F. Beerendonk, C.H.M. Hofman-Caris, Degradation of pharmaceuticals in UV (LP)/H_2O_2 reactors simulated by means of kinetic modeling and computational fluid dynamics (CFD), Water Res., 75 (2015) 11–24.

[24] B.A. Wols, D.J.H. Harmsen, E.F. Beerendonk, C.H.M. Hofman-Caris, Predicting pharmaceutical degradation by UV (MP)/H_2O_2 processes: a kinetic model, Chem. Eng. J., 263 (2015) 336–345.

[25] B.A. Wols, C.H.M. Hofman-Caris, Review of photochemical reaction constants of organic micropollutants required for UV advanced oxidation processes in water, Water Res., 46 (2012) 2815–2827.

[26] F. Yuan, C. Hu, X.X. Hu, J.H. Qu, M. Yang, Degradation of selected pharmaceuticals in aqueous solution with UV and UV/H_2O_2, Water Res., 43 (2009) 1766–1774.

[27] D. Palma, A.B. Prevot, M. Brigante, D. Fabbri, G. Magnacca, C. Richard, G. Mailhot, R. Nisticò, New insights on the photodegradation of caffeine in the presence of bio-based substances-magnetic iron oxide hybrid nanomaterials, Materials (Basel), 11 (2018) 1–17.

[28] N. Liu, W.Y. Huang, M.Q. Tang, C.C. Yin, B. Gao, Z.M. Li, L. Tang, J.Q. Lei, L.F. Cui, X.D. Zhang, In-situ fabrication of needle-shaped MIL-53(Fe) with 1T-MoS_2 and study on its enhanced photocatalytic mechanism of ibuprofen, Chem. Eng. J., 359 (2019) 254–264.

[29] X.D. Zhang, Y. Yang, W.Y. Huang, Y.Q. Yang, Y.X. Wang, C. He, N. Liu, M.H. Wu, L. Tang, g-C_3N_4/UiO-66 nanohybrids with enhanced photocatalytic activities for the oxidation of dye under visible light irradiation, Mater. Res. Bull., 99 (2018) 349–358.

[30] J. Schneider, M. Matsuoka, M. Takeuchi, J.L. Zhang, Y. Horiuchi, M. Anpo, D.W. Bahnemann, Understanding TiO_2 photocatalysis: mechanisms and materials, Chem. Rev., 114 (2014) 9919–9986.
[31] IUPAC, Compendium of Chemical Terminology: Gold Book, International Union of Pure and Applied Chemistry, Royal Society of Chemistry, Cambridge, UK, 2014, p. 1670.
[32] L.L. Shao, S.K. Yang, W.K. Wang, Nano-Titanium Dioxide Mediate Photocatalytic Degradation of Caffeine, Environmental Science and Engineering College, Chang'an University, Xi'an, China, 2012.
[33] C. Indermuhle, M.J. Martín de Vidales, C. Sáez, J. Robles, P. Cañizares, J.F. García-Reyes, A. Molina-Díaz, C. Comninellis, M.A. Rodrigo, Degradation of caffeine by conductive diamond electrochemical oxidation, Chemosphere, 93 (2013) 1720–1725.
[34] P. Atkins, J. de Paula, Physical Chemistry, W.H. Freeman and Co., New York, 2006.
[35] S.L. Cole, J.W. Wilder, Gas phase decomposition by the Lindemann mechanism, SIAM J. Appl. Math., 51 (1998) 1489–1497.
[36] T. Batakliev, V. Georgiev, M. Anachkov, S. Rakovsky, G.E. Zaikov, Ozone decomposition, Phys. Chem. Res. Eng. Appl. Sci. Vol. 1 Princ. Technol. Implic., 7 (2015) 273–304.
[37] C. Chieh, Chemistry LibreTexts - Steady-State Approximation, Department of Education Open Textbook Pilot Project, UC Davis Library, California, 2016. Available at: https://chem.libretexts.org.
[38] S.S. Brown, H. Stark, A.R. Ravishankara, Applicability of the steady state approximation to the interpretation of atmospheric observations of NO_3 and N_2O_5, J. Geophys. Res., 108 (2003) 4539, doi:10.1029/2003JD003407.
[39] E.H. Flach, S. Schnell, Use and abuse of the quasi-steady-state approximation, Syst. Biol. (Stevenage), 153 (2006) 187–191.
[40] T. Turányi, A.S. Tomlin, M.J. Pilling, On the error of the quasi-steady-state approximation, J. Phys. Chem., 97 (1993) 163–172.
[41] V. Viossat, R.I. Ben-Aim, A test of the validity of steady state and equilibrium approximations in chemical kinetics, J. Chem. Educ., 70 (1993) 732.
[42] J.K. Kim, K. Josić, M.R. Bennett, The validity of quasi-steady-state approximations in discrete stochastic simulations, Biophys. J., 107 (2014) 783–793.
[43] F. Di Giacomo, A short account of RRKM theory of unimolecular reactions and of marcus theory of electron transfer in a historical perspective, J. Chem. Educ., 92 (2015) 476–481.

Appendix A

A1. Heterogeneous photo-catalysis of caffeine

As mentioned above, simplified kinetic processes based on "rate determination step" or "steady state" approximations, as Michaelis-Menten, N_2O_5 [34] Lindemann–Hinshelwood [35], or ozone degradation [36] mechanisms can be useful to understand the elementary steps of a complex process. In order to try to elucidate whether light excitation occurs before or after the adsorption we tested the following simplified processes described below.

Process "α" can be defined by the following elementary steps:

- adsorption of caffeine (*F*) on TiO_2 (*T*) forming a complex (*FT*) with rate coefficient $k_{\alpha 1:}$

$$F + T \rightarrow FT \quad \text{[Process } \alpha 1\text{]} \tag{A1}$$

The complex *FT* can disintegrate back to caffeine, with a rate coefficient $k_{\alpha -1}$:

$$FT \rightarrow F + T \quad \text{[Process } \alpha - 1\text{]} \tag{A2}$$

- absorb a suitable photon (hν) to become an excited caffeine–TiO_2 complex (*FT**) with a rate coefficient $k_{\alpha 2}$:

$$FT^* + h\upsilon \rightarrow FT^* \quad \text{[Process } \alpha 2\text{]} \tag{A3}$$

- that might relax by internal conversion

$$FT^* \rightarrow FT \quad \text{[Process } \alpha 3\text{]} \tag{A4}$$

with a rate coefficient k_3,

- or yield degradation products *P*, with a rate coefficient k_4, leaving behind free TiO_2:

$$FT^* \rightarrow P + T \quad \text{[Process } \alpha 4\text{]} \tag{A5}$$

It can be seen that this process has two intermediates: *FT* and *FT**. Assuming that processes are governed by a collision mechanism, and thus the order of each component in an elementary step is a function of its stoichiometric value, then the rate of formation of *FT* which is created by process [α1] (Eq. (A1)) and [α3] (Eq. (A4)), and disintegrated by processes [α–1] (Eq. (A2)) and [α2] (Eq. (A3)) will be:

$$\frac{d\left[FT\right]}{dt} = k_{\alpha 1}\left[F\right]\left[T\right] + k_3\left[FT^*\right] - k_{\alpha -1}\left[FT\right] - k_{\alpha 2}\left[FT\right]\left[h\upsilon\right] \tag{A6}$$

A similar equation can be given for the rate of formation of the excited complex, *FT**, which is formed in process [α2] (Eq. (A3)) and disintegrated by processes [α3] (Eq. (A4)) and [α4] (Eq. (A5)):

$$\frac{d\left[FT^*\right]}{dt} = k_{\alpha 2}\left[FT\right]\left[h\upsilon\right] - k_3\left[FT^*\right] - k_4\left[FT^*\right] \tag{A7}$$

The steady-state approximation, based on the assumption that intermediates are consumed as quickly as generated [37], has been widely used to simplify kinetic processes in several disciplines [38,39]. Even though the validity of such approximation is questioned [39,40], and methods to evaluate such validity were developed [41,42], it still "remains a powerful tool for the simplification of reaction structures" in kinetic simulations [40]. Applying in this case, the "steady-state approximation" will mean that the concentration of the intermediate components remain constant, thus, rates in Eqs. (A6) and (A7) will be zero. This will yield estimates for the concentration of the complex and activated complex:

$$\left[FT\right] = \frac{k_{\alpha 1}\left[F\right]\left[T\right] + k_3\left[FT^*\right]}{k_{\alpha -1} + k_{\alpha 2}\left[h\upsilon\right]} \tag{A8}$$

$$\left[FT^*\right]=\frac{k_{\alpha 2}\left[FT\right]\left[h\upsilon\right]}{k_3+k_4}=\frac{k_{\alpha 2}\left[h\upsilon\right]}{k_3+k_4}\frac{k_{\alpha 1}\left[F\right]\left[T\right]+k_3\left[FT^*\right]}{k_{\alpha -1}+k_{\alpha 2}\left[h\upsilon\right]} \quad \text{(A9)}$$

For the sake of simplicity, we can use the following notations: $k_{X'} = (k_3 + k_4)k_{\alpha-1}$ and $k_{Y'} = (k_3 + k_4)k_{\alpha 2}$. Such notations will make Eq. (A9):

$$\left[FT^*\right]=\frac{k_{\alpha 2}k_{\alpha 1}\left[h\upsilon\right]\left[F\right]\left[T\right]+k_3k_{\alpha 2}\left[h\upsilon\right]\left[FT^*\right]}{k_{X'}+k_{Y'}\left[h\upsilon\right]} \quad \text{(A10)}$$

which after reordering to isolate $[FT^*]$ yields:

$$\left[FT^*\right]=\frac{k_{\alpha 2}k_{\alpha 1}\left[h\upsilon\right]\left[T\right]}{k_{X'}+k_{Y'}\left[h\upsilon\right]-k_3k_{\alpha 2}\left[h\upsilon\right]}\left[F\right] \quad \text{(A11)}$$

Since the overall rate process is the rate of formation of the products, then we may elaborate from Eq. (A5), obtaining:

$$\upsilon=\frac{d\left[P\right]}{dt}=k_4\left[FT^*\right]=\frac{k_4k_{\alpha 2}k_{\alpha 1}\left[h\upsilon\right]\left[T\right]}{k_{X'}+k_{Y'}\left[h\upsilon\right]-k_3k_{\alpha 2}\left[h\upsilon\right]}\left[F\right] \quad \text{(A12)}$$

According to Eq. (A12), the proposed process should be first order for caffeine at all concentrations. At high light rates, when $k_{X'}/(k_{Y'}-k_3k_{\alpha 2}) \ll \left[h\upsilon\right]$ the proposed process will apparently become pseudo-zero-order on light intensity.

Process "γ" can be defined by the following elementary steps:

- Excitation of TiO_2 forming an excited catalyst (T^*) with a rate coefficient $k_{\gamma 1}$:

$$T+h\upsilon\rightarrow T^* \quad \left[\text{Process } \gamma 1\right] \quad \text{(A13)}$$

which may relax by the opposite reaction with a rate coefficient $k_{\gamma-1}$:

$$T^*\rightarrow T \quad \left[\text{Process } \gamma-1\right] \quad \text{(A14)}$$

- or may combine with caffeine forming an excited complex FT^* with a rate coefficient $k_{\gamma 2}$:

$$T^*+F\rightarrow FT^* \quad \left[\text{Process } \gamma 2\right] \quad \text{(A15)}$$

- The next steps are similar to the previous path. The excited complex might relax by internal conversion, following process [α3] (Eq. (A4)) and eventually releasing F and T with a rate coefficient k_3, or by forming products P following process [α4] (Eq. (A5)), with a rate coefficient k_4, leaving behind free TiO_2.

As before, such a process has two intermediates: excited catalyst T^* and excited complex FT^*. The rate of formation of T^*, which is created by process [γ1] (Eq. (A13)) and disintegrated by processes [γ–1] (Eq. (A14)) and [γ2] (Eq. (A15)) will be:

$$\frac{d\left[T^*\right]}{dt}=k_{\gamma 1}\left[h\upsilon\right]\left[T\right]-k_{\gamma-1}\left[T^*\right]-k_{\gamma 2}\left[T^*\right]\left[F\right] \quad \text{(A16)}$$

A similar equation for the rate of formation of the excited complex, FT^*, which is formed in process [γ2] (Eq. (A15)) and disintegrated by processes [α3] (Eq. (A4)) and [α4] (Eq. (A5)) is:

$$\frac{d\left[FT^*\right]}{dt}=k_{\gamma 2}\left[T^*\right]\left[F\right]-k_3\left[FT^*\right]-k_4\left[FT^*\right] \quad \text{(A17)}$$

Again, assuming a "steady-state" mechanism will yield values for the suspension of the activated catalyst and activated complex:

$$\left[T^*\right]=\frac{k_{\gamma 1}\left[h\upsilon\right]\left[T\right]}{k_{\gamma-1}+k_{\gamma 2}\left[F\right]} \quad \text{(A18)}$$

$$\left[FT^*\right]=\frac{k_{\gamma 2}\left[T^*\right]\left[F\right]}{k_3+k_4}=\frac{k_{\gamma 2}\left[F\right]}{k_3+k_4}\frac{k_{\gamma 1}\left[h\upsilon\right]\left[T\right]}{k_{\gamma-1}+k_{\gamma 2}\left[F\right]} \quad \text{(A19)}$$

Since the overall rate process is the rate of formation of the products, then we may elaborate from Eq. (A5), obtaining:

$$\upsilon=\frac{d\left[P\right]}{dt}=k_4\left[FT^*\right]=\frac{k_4k_{\gamma 2}k_{\gamma 1}\left[h\upsilon\right]\left[T\right]\left[F\right]}{\left(k_3+k_4\right)\left(k_{\gamma-1}+k_{\gamma 2}\left[F\right]\right)} \quad \text{(A20)}$$

As in process "α", we may, for the sake of simplicity, use the following notations: $k_X = (k_3 + k_4)k_{\gamma-1}$, $k_Y = (k_3 + k_4)k_{\gamma 2}$. Such notations will make Eq. (A20):

$$\upsilon=\frac{d\left[P\right]}{dt}=k_4k_{\gamma 1}k_{\gamma 2}\left[h\upsilon\right]\left[T\right]\frac{\left[F\right]}{\left(k_X+k_Y\left[F\right]\right)} \quad \text{(A21)}$$

And from Eq. (A21) we can easily deduce that large concentrations of caffeine might lead to $k_Y[F] \gg k_X$, Under these conditions, the process will behave as a pseudo-zero-order on F:

$$k_Y\left[F\right]\gg k_X\rightarrow \upsilon=k_4k_{\gamma 1}k_{\gamma 2}\left[h\upsilon\right]\left[T\right]\frac{\left[F\right]}{\left(k_X+k_Y\left[F\right]\right)}\approx k_4k_{\gamma 1}k_{\gamma 2}\left[h\upsilon\right]\left[T\right]\frac{\left[F\right]}{\left(k_Y\left[F\right]\right)}=\frac{k_4k_{\gamma 1}k_{\gamma 2}}{k_Y}\left[h\upsilon\right]\left[T\right] \quad \text{(A22)}$$

On the other hand, at very low caffeine concentrations, when $k_Y[F] \ll k_X$, the rate will become pseudo-first-order on caffeine:

$$k_Y\left[F\right]\gg k_X\rightarrow \upsilon=k_4k_{\gamma 1}k_{\gamma 2}\left[h\upsilon\right]\left[T\right]\frac{\left[F\right]}{\left(k_X+k_Y\left[F\right]\right)}\approx \frac{k_4k_{\gamma 1}k_{\gamma 2}}{k_Y}\left[h\upsilon\right]\left[T\right]\left[F\right] \quad \text{(A23)}$$

whereas between those end values, the behavior will be a function of the transient state.

In order to obtain full description additional more accurate models as RRKM (Rice, Ramsperger, Kassel, Marcus) theory [43] should be required. However, despite the limitation of the simplified processes described above, it appears that light excitation of the caffeine-TiO_2 (mechanism "α") leads to a first-order process on caffeine at all concentrations, whereas light excitation of TiO_2 followed by adsorption (mechanism "γ") leads to the measured effect: first order and zero order at low and high caffeine concentrations, respectively.

Appendix B

B1. Specific rate laws for pseudo-zero- and first-order kinetics

In cases where the rate is independent of the contaminating compound concentration, the process is defined as "pseudo-zero-order" and can be expressed as:

$$A_t = A_0 - k_{app}t \tag{B1}$$

thus its half-life time can be obtained by:

$$t_{1/2} = \frac{\left[A\right]^0}{2k_{app}} = \frac{1}{2k_{app}} \tag{B2}$$

whereas in a "pseudo-first-order" process, the reaction proceeds at a rate that depends linearly on the concentration of the contaminating compound and it can be expressed as:

$$\frac{d\left[A\right]}{dt} = -k_{app}\left[A\right]^1 = -k_{app}\left[A\right] \tag{B3}$$

thus its half-life can be described by:

$$t_{1/2} = \frac{-\ln\left(1/2\right)}{k_{app}} = \frac{\ln 2}{k_{app}} \tag{B4}$$

Supplementary information

Table S1
Experimental plan and results

Exp. #	Caffeine concentration ($\mu g\ L^{-1}$)	H_2O_2 concentration ($\mu mol\ L^{-1}$)	TiO_2 suspension ($\mu g\ L^{-1}$)	UV-C dose β	Apparent Rate coefficient k_{app} (min^{-1})	Half-life time $t_{½}$ (min)
1	19,600	0	–	1	~0	∞
2	19,600	163.0	–	0	~0	∞
3	19,600	16.30	–	1	0.0117	42.73
4	19,600	40.75	–	1	0.0396	12.62
5	19,600	81.50	–	1	0.0607	8.24
6	19,600	163.0	–	1	0.0918	5.45
7	19,600	163.0	–	0.5	0.0498	10.04
8	19,600	163.0	–	0.25	0.0256	19.53
9	19,600	163.0	–	0.125	0.0142	35.21
10	19,600	81.50	–	0.5	0.0358	13.97
11	19,600	81.50	–	0.25	0.0195	25.64
12	19,600	81.50	–	0.125	0.0095	52.63
13	19,600	40.75	–	0.5	0.0180	27.77
14	19,600	40.75	–	0.25	0.0127	39.37
15	19,600	40.75	–	0.125	0.0068	73.52
16	19,600	16.30	–	0.5	0.0069	72.46
17	19,600	16.30	–	0.25	0.0048	104.1
18	19,600	–	10	0	~0	∞
19	19,600	–	1	1	0.0052	96.15
20	19,600	–	5	1	0.0108	46.29
21	19,600	–	10	1	0.0156	32.05
22	19,600	–	20	1	0.0216	23.14
23	19,600	–	30	1	0.0280	17.86
24	19,600	–	50	1	0.0399	12.53
25	19,600	–	100	1	0.0571	8.76
26	19,600	–	20	0.5	0.0160	31.25
27	19,600	–	20	0.25	0.0115	43.48
28	19,600	–	20	0.125	0.0080	62.50
29	19,600	–	30	0.125	0.0103	48.54
30	19,600	–	50	0.5	0.0256	19.53
31	19,600	–	50	0.25	0.0181	27.62
32	19,600	–	50	0.125	0.0138	36.26
33	19,600	–	100	0.5	0.0373	13.40
34	19,600	–	100	0.25	0.0266	18.80
35	9,800	–	10	1	0.0342	14.62
36	9,800	–	20	1	0.0473	10.57
37	9,800	–	30	1	0.1340[a]	5.17
38	9,800	–	100	1	0.1871[a]	3.70
39	9,800	–	200	1	0.2084[a]	3.32
40	19,600	–	200	1	0.1078[a]	6.43
41	14,700	–	200	1	0.1453[a]	4.77
42	24,500	–	200	1	0.0777[a]	8.98

[a]First-order reaction